

## Circularly polarized luminescence under near-UV excitation and structural elucidation of a Eu complex

Received 00th January 20xx,  
Accepted 00th January 20xx

Francesco Zinna,<sup>a</sup> Claudio Resta,<sup>ab</sup> Sergio Abbate,<sup>c</sup> Ettore Castiglioni,<sup>cd</sup> Giovanna Longhi,<sup>c</sup> Placido Mineo,<sup>e</sup> Lorenzo Di Bari<sup>\*a</sup>

DOI: 10.1039/x0xx00000x

www.rsc.org/

**A new chiral diketonate ligand based on carvone binds early lanthanides. The Eu complex displays highly circularly polarized ( $g_{lum} = 0.82$ ) red luminescence under near-UV excitation at solid state. This is the first report of such CPL activity at solid state with a rigorous protocol to exclude artifacts. Paramagnetic NMR revealed nature and structure of the active species.**

Lanthanide luminescence has found widespread applications for lighting<sup>1, 2</sup> and for electronic devices,<sup>3</sup> in security inks,<sup>4, 5</sup> in stains and labels for *in vivo* or *ex vivo* imaging or microscopy,<sup>6, 7</sup> just to cite a few examples. This is true for inorganic compounds, as well as for complexes with organic ligands. In this second option the ligand has two primary functions: **1**) to chelate the Ln<sup>3+</sup>, making it soluble and stable in the desired environment; **2**) to provide the so-called antenna effect, i.e. to capture excitation (for example absorbing high energy light) and pass it onto the Ln<sup>3+</sup>, which thereupon emits a photon. As a further bonus, the ligand lends itself to a practically infinite set of manipulations and decorations, typical of organic chemistry, and thus modulate chemical, optical, and electronic properties of the complex.<sup>8</sup>

In our present work, we addressed two main issues: **1**) we wanted to push the excitation wavelength toward visible light, in order to avoid undesirable (far)-UV irradiation; **2**) we sought high circularly polarized luminescence (CPL), as conveniently measured by the so-called dissymmetry factor  $g_{lum}$

$$g_{lum} = \frac{(I_L - I_R)}{\frac{1}{2}(I_L + I_R)}$$

Where  $I_L$  and  $I_R$  are the left and right polarized emission intensities respectively (with  $2 \geq g_{lum} \geq -2$ ).

<sup>a</sup> Dipartimento di Chimica e Chimica Industriale, Università di Pisa, Via Moruzzi 13, I-56126, Pisa, Italy

<sup>b</sup> Dipartimento di Chimica "Ugo Schiff", Via della Lastruccia 3, 50019 Sesto F.no (FI), Italy

<sup>c</sup> Dipartimento di Medicina Molecolare e Traslazionale, Università di Brescia, Viale Europa 11, 25123, Brescia Italy

<sup>d</sup> JASCO Europe, Via Cadorna 1, 23894 Cremella (LC), Italy

<sup>e</sup> Dipartimento di Scienze Chimiche, Viale Andrea Doria, 6, 95123 Catania, Italy.

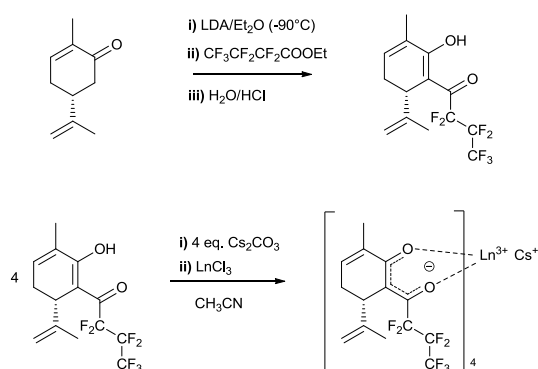
Feature **1**) is desirable, because typical excitation wavelengths are 330 nm or below, which is hard on eyes and skin and induces serious damage to tissues (limiting *in vivo* imaging applications). In any case the extremely large shift between absorption and emission wavelengths of Ln complexes ensures that there would be no interference between absorption and emission processes. Feature **2**) will respond to a need of encoding information in the form of light polarization which may find application e.g. for the development of 3D-displays,<sup>9</sup> for open-space communications, or for anti-counterfeiting labeling systems. Lanthanide chiral complexes have proven ideal candidates as emitters of circularly polarized light, since they can often attain  $g_{lum}$  2-3 order of magnitude higher than the ones obtained with purely organic molecules.<sup>10-12</sup> Among several diketonates with outstanding luminescence and CPL activity,<sup>13-18</sup> the most notable one is the camphorate complex reported by Kaizaki et al. with a  $g_{lum}$  of 1.38.<sup>19</sup>

With this in mind, we chose carvone, a commercially available chiral  $\alpha,\beta$ -unsaturated ketone which naturally occurs in both enantiomers. A Claisen reaction with ethyl perfluorobutyrate as the partner yielded a  $\beta$ -diketone. In order to assess the suitability of the product for most practical applications, it is necessary to test its CPL at the solid state. This kind of measurements is still uncommon, maybe due to the fact that special experimental care should be taken to avoid the occurrence of artifacts.<sup>20-22</sup>

The ligand heptafluorobutyrylcarvone<sup>23</sup> (hfbcvH) was readily synthesized, acylating the carvone enolate with ethyl heptafluorobutyrate (see **Scheme 1**).<sup>†</sup> It is noteworthy that  $\lambda_{max}$  for the lowest lying transition of the anion is 370 nm, some 40 nm redshifted compared to common diketonates (Figure S1). Both the neutral and anionic form of the ligand display a circular dichroism spectrum (Figure S2).

At first, for the metalation, we employed a biphasic system using triethylamine as the base and LnCl<sub>3</sub>,<sup>24</sup> unfortunately these conditions yielded a mixture of two lanthanide adducts (see below), while we observed a certain decomposition of the ligand to yield back carvone and heptafluorobutyrate, due to a retro-Claisen process. Using instead a stoichiometric quantity

of  $\text{Cs}_2\text{CO}_3$  as the base in anhydrous acetonitrile (**Scheme 1**),  $^1\text{H-NMR}$  demonstrated the presence of one paramagnetic compound, although in presence of a small quantity of unreacted ligand. These anhydrous conditions prevented the retro-Claisen decomposition. Upon complexation, the  $\pi \rightarrow \pi^*$  diketonate band undergoes a blue shift of about 15 nm (Figure S1 and S3). Using  $\text{Na}^+$  and  $\text{K}^+$  carbonates, the reactions were sluggish and were discarded. The main reason of this drawback can be ascribed to the poor solubility of sodium and potassium carbonates compared to  $\text{Cs}_2\text{CO}_3$ . Before discussing the nature of the  $\text{Ln}^{3+}$  species formed, we shall describe the foremost optical properties of the Eu-derivative, which were the target of our investigation.



**Scheme 1:** Synthesis of heptafluorobutrylcarvone (hfbcvH) and  $\text{Cs}[\text{Ln}(\text{hfbcv})_4]$  complexes.

Figure S4, S5 display the emission in acetonitrile solution and of a quartz window deposition. Excitation spectrum (Figure S6) shows that, although maximum excitation is obtained with  $\lambda_{\text{exc}} = 370 \text{ nm}$ , much longer wavelengths would profitably be used, possibly extending to 420 nm. Identity of the emission spectra of solution and deposition is the first demonstration we encounter that the emitting species must be similar in both states.

A further evidence is given by the similarity of circular dichroism (CD) spectra (**Figure 1**) taken on the  $\text{CH}_3\text{CN}$  solution and on a quartz deposition. This indicates that the arrangement of ligands is not particularly different in the two media.<sup>17</sup>

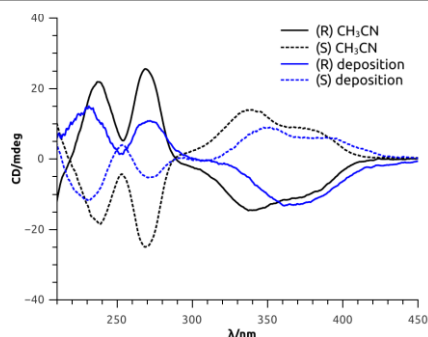


**Figure 1:** CD spectra of  $\text{Cs}[\text{Eu}(\text{hfbcv})_4]$  (R/S dashed/continuous lines) in  $\text{CH}_3\text{CN}$  solution (black) and on quartz plate depositions (blue).

The CPL spectrum of the acetonitrile solution is depicted in Figure S7. We may observe that for the two enantiomers of the ligand the spectra are mirror image, as expected, and we should also mention that the CPL data are completely consistent and reproducible from one sample to the next, also starting from completely new preparations of the ligand. The magnetically-allowed transition  $^5D_0 \rightarrow ^7F_1$  at about 594 nm displays the respectable  $g$ -value of 0.15. As it often occurs, it has a rotational strength almost equal and opposite to the one of  $^5D_0 \rightarrow ^7F_2$  around 612 nm. Because this has electric-dipole character, it is associated with a strong luminescence and it is indeed the most prominent feature of the total emission spectrum. Accordingly, its  $g$ -value is much smaller.

Things become much more interesting when we switch to the solid state (deposition of a few drops of the  $\text{CH}_3\text{CN}$  solution followed by slow solvent evaporation). In this case, we find the CPL spectrum of **Figure 2**, which displays much stronger signals. In this case, the  $g$ -value at 594 nm reaches 0.82. To the very best of our knowledge, this value is one of the highest ever recorded<sup>25, 26</sup> and one of the first reports of outstanding CPL properties of chiral lanthanide complexes at solid state. The reproducibility of the data over several depositions, starting from different preparations of the complexes (Figure S8), the absence of fluorescence linear anisotropy signals and above all the almost perfect mirror-image CPL of the two enantiomers rule out the occurrence of artifacts (Figure 2). The experimental set-up employed to record the CPL spectra is described in the ESI. We notice that the solid state luminescence is enhanced with respect to the solution one, this is in agreement with previous observations,<sup>27</sup> although no ultimate explanation has been put forward. Possibly, crystal packing on one hand and solvation on the other may account for both total luminescence and CPL enhancement in solid state samples.

The  $^5D_0 \rightarrow ^7F_0$  transition at 583 nm is a single sharp band (see Figure S4, S5), in both solution and solid state, this is consistent with the presence of only one Eu species in both cases.

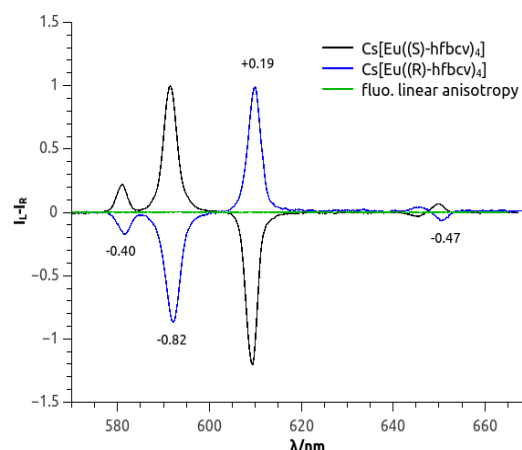


**Figure 2:** CPL spectra of  $\text{Cs}[\text{Eu}(\text{S})\text{-hfbcv})_4]$  (black) and  $\text{Cs}[\text{Eu}(\text{R})\text{-hfbcv})_4]$  (blue) on a quartz plate upon irradiation at 370 nm, with calculated  $g_{\text{lum}}$  values and fluorescence linear anisotropies (green).

The promising features of the CPL make us prospect immediate applications: in the first place, one can envisage a security ink which can emit red circularly polarized light under blue-light illumination, secondly, our recent experience with circularly polarized light emitting devices (CP-LED)<sup>28</sup> make us wonder if the ease of excitation of the ligand will have consequences in electroluminescence, as it does with photoexcitation. For these reasons, we attempted by all means to isolate the active species, which unfortunately resulted elusive. This is possibly due to the unavoidable presence of residual ligand. Willing to get as much information as possible on the active species and given our ability to solve solution structures based on paramagnetic NMR,<sup>29</sup> we addressed the following questions: **1)** what is the CPL-active species; **2)** determine its solution structure; **3)** what other species are present, possibly in equilibrium with the most abundant one.

In order to characterize the product we obtained and to give an answer to point 3, we acquired MALDI-TOF mass spectra of Cs[Eu(hfbcv)<sub>4</sub>], in CH<sub>2</sub>Cl<sub>2</sub> solution in both positive (Figure S17) and in negative (Figure S18) mode. The positive MALDI-TOF (Figure S16) shows a peak at *m/z* 1666.5, attributed to the Cs[Eu(hfbcv)<sub>4</sub>] (detected as [M]H<sup>+</sup>) species. The low quality of the spectrum was due to a low ion efficiency of the analyzed molecular systems. On the other hand, the presence of the *tetrakis* compound ([Eu(hfbcv)<sub>4</sub>]<sup>-</sup>) is much better appreciated by negative MALDI-TOF spectrum (Figure S18) which displays an intense peak at *m/z* 1532.6. This peak is ascribed to the anionic species resulting from the cation (Cs<sup>+</sup>) loss from Cs[Eu(hfbcv)<sub>4</sub>] during the MALDI desorption process. The inset of Figure S17 provides a comparison between the experimental isotopic cluster peaks at *m/z* 1532.6 with the expected simulated isotopic distribution for [Eu(hfbcv)<sub>4</sub>]<sup>-</sup>. The same spectrum shows also a signal at *m/z* 1187.3 and a less intense peak at *m/z* 345.5 attributed to Eu(hfbcv)<sub>3</sub> and to the free ligand hfbcv<sup>-</sup> respectively.

The <sup>1</sup>H-NMR spectra of all synthesized Cs[Ln(hfbcv)<sub>4</sub>] complexes (Ln= Ce, Pr, Nd, Eu, Tb) in CD<sub>3</sub>CN solution showed only one set of paramagnetically shifted proton resonances, compatible with the hfbcv resonances, indicating that the only paramagnetic species present has a C<sub>4</sub> symmetry. The narrow lines suggested that the complexes do not undergo conformational rearrangements in slow or intermediate exchange regime on the NMR time scale under the investigated conditions.<sup>30</sup>

We assigned the NMR spectra through homo- and heterocorrelation experiments and we extracted the pseudocontact shifts (see ESI). The analysis of these shifts indicates isostructurality along the investigated portion of the series (Figure S10).

Taking advantage of the structural information contained in pseudocontact shifts, we were able to assess a structure for Cs[Ln(hfbcv)<sub>4</sub>] compounds in acetonitrile solution (Figure 3), using the routine PERSEUS,<sup>30, 31</sup> starting from a DFT level pre-optimized ligand structure and imposing a C<sub>4</sub> symmetry for consistency with experimental data. Beside <sup>1</sup>H shifts, we included in the calculation pseudocontact <sup>13</sup>C shifts, relaxation rates and an estimated Ln-O distance (2.4 Å),<sup>32</sup> as additional

boundaries. The dihedral angle between the ring and the isopropenyl group remained unchanged with respect to the DFT structure of the ligand used as the input of PERSEUS.

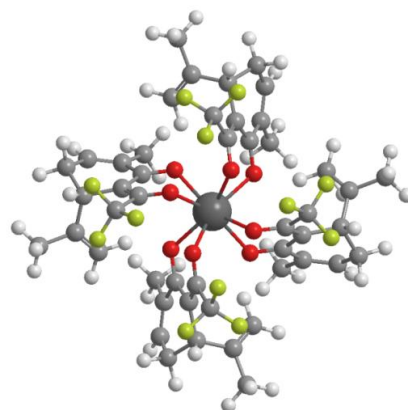


**Figure 3:** Solution (CD<sub>3</sub>CN) structure of Cs[Ln((R)-hfbcv)<sub>4</sub>] obtained from PERSEUS. Since the perfluoropropyl chains could not be included in the calculation, they are here represented as trifluoromethyl groups for visual purpose only.

The PERSEUS output pointed out that the structure is a twisted square antiprism (TSA) with a twist angle of 22.9° meaning that the coordination polyhedron itself is chiral and it may account for the high luminescence dissymmetry factor that we observed.<sup>33</sup> The bite angle is 73.0° which is especially small and definitely does not allow for water coordination to the axial position. This is consistent with the observation that the residual HDO signal in the NMR spectrum of Cs[Ln(hfbcv)<sub>4</sub>] systematically falls at 2.13 ppm, i.e. at the usual chemical shift of water in acetonitrile and it does not experience any Ln-dependent dia- or paramagnetic shift, as one would expect in the case of water participating in metal coordination.

Using a similar argument, we observed that <sup>133</sup>Cs-NMR spectra of Cs[La(hfbcv)<sub>4</sub>] and Cs[Pr(hfbcv)<sub>4</sub>] are practically identical, i.e. there is no detectable paramagnetic shift of <sup>133</sup>Cs (see also ESI).

This means that Cs<sup>+</sup> does not occupy a precise geometric position with respect to Pr<sup>3+</sup> magnetic anisotropy tensor. Consequently, we do not deal with a true heterobimetallic complex, but rather with an anionic complex [Ln(hfbcv)<sub>4</sub>]<sup>-</sup>, which is remarkably different from what had been deduced for the apparently similar camphorate system CsLn(hfbc)<sub>4</sub>.

All the investigated complexes show the presence of variable quantities of free ligand in solution and the exchange equilibrium between free and bound ligands in the *tetrakis* species is active. This could be demonstrated by means of a EXSY spectra which displays exchange cross peaks between all paramagnetically shifted signals and those of the free ligand.

The nature of this anionic *tetrakis* species can be best appreciated by contrast with the *tris* Ln(hfbcv)<sub>3</sub>, which we found present when using a different synthesis protocol (i.e. a biphasic system). In this case, EXSY experiments reveal that the *tetrakis* and *tris* forms are in slow exchange on the NMR timescale: this ensures that if the *tris* complex were present in the product of Cs<sub>2</sub>CO<sub>3</sub> protocol, we would see its fingerprint in the NMR spectrum. Standard bidimensional NMR techniques

allowed us to assign the resonances related to  $\text{Ln}(\text{hfbcv})_3$  ( $\text{Ln}=\text{Pr}, \text{Eu}$ ). We noticed that only in the samples containing the *tris* complex, the water resonance was shifted upfield indicating an axial coordination to the lanthanide, in  $\text{Ln}(\text{hfbcv})_3$ , which, unlike the *tetrakis* species, is coordinatively unsaturated. The different behaviour of the  $[\text{Ln}(\text{hfbcv})_4]^-$  and  $\text{Ln}(\text{hfbcv})_3$  with respect to axial coordination was further investigated by testing them with DMSO which has a strong affinity for  $\text{Ln}^{3+}$ . Indeed, upon adding increasing quantities of DMSO to the mixture of *tris/tetrakis* Pr compounds, the water resonance recovered its standard shift at 2.13 ppm, DMSO resonance resulted shifted upfield, in accordance with axial coordination to Pr. Moreover, all the resonances assigned to the *tris* species were affected by the DMSO addition, while those of the *tetrakis* complex remained unchanged (**Figure 4**).

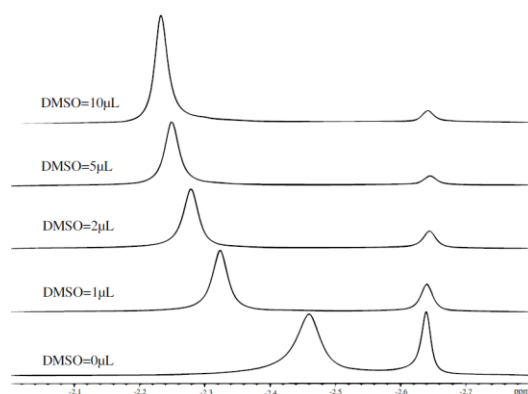


**Figure 4:**  $\text{Me}_9$  (see **Scheme 1**) resonances for  $\text{Pr}(\text{hfbcv})_3$  (left signals) and  $[\text{Pr}(\text{hfbcv})_4]^-$  (right signals) at increasing concentrations of DMSO.

We observed that during the titration, the molar ratio *tris/tetrakis* increased, suggesting that the *tris* species is stabilized by the axial coordination of DMSO. A quantitative analysis is reported in the ESI (Table S5 and Figure S15). In conclusion we synthesized a new Eu species, with near UV excitation and highly circularly polarized photoluminescence at solid state. We also investigated the structure of the series of complexes of early lanthanides through NMR spectroscopy.

## References and notes

- <sup>†</sup> hfbcvH was already reported in reference [23] to be employed as the stationary phase in a column for chiral chromatography, however the authors do not report any detailed characterization.
1. J.-C. G. Bünzli, S. Comby, A.-S. Chauvin and C. D. B. Vandevyver, *J. Rare Earths*, 2007, **25**, 257-274.
2. K. Binnemans, *Chem. Rev.*, 2009, **109**, 4283-4374.
3. R. C. Evans, P. Douglas and C. J. Winscom, *Coord. Chem. Rev.*, 2006, **250**, 2093-2126.
4. J. Andres, R. D. Hersch, J.-E. Moser and A.-S. Chauvin, *Adv. Funct. Mater.*, 2014, **24**, 5029-5036.
5. J.-C. G. Bünzli and S. V. Eliseeva, *Chem. Sci.*, 2013, **4**, 1939-1949.
6. E. G. Moore, A. P. S. Samuel and K. N. Raymond, *Acc. Chem. Res.*, 2009, **42**, 542-552.
7. C. P. Montgomery, B. S. Murray, E. J. New, R. Pal and D. Parker, *Acc. Chem. Res.*, 2009, **42**, 925-937.
8. J.-C. G. Bünzli, *Coord. Chem. Rev.*, 2015, **293-294**, 19-47.
9. R. Farshchi, M. Ramsteiner, J. Herfort, A. Tahraoui and H. Grahn, *Appl. Phys. Lett.*, 2011, **98**, 162508.
10. F. Zinna and L. Di Bari, *Chirality*, 2015, **27**, 1-13.
11. S. Abbate, G. Longhi, F. Lebon, E. Castiglioni, S. Superchi, L. Pisani, F. Fontana, F. Torricelli, T. Caronna and C. Villani, *J. Phys. Chem. C*, 2014, **118**, 1682-1695.
12. G. Longhi, S. Abbate, G. Mazzeo, E. Castiglioni, P. Mussini, T. Benincori, R. Martinazzo and F. Sannicolò, *J. Phys. Chem. C*, 2014, **118**, 16019-16027.
13. A. Zaim, N. D. Favera, L. Guenee, H. Nozary, T. N. Y. Hoang, S. V. Eliseeva, S. Petoud and C. Piguet, *Chem. Sci.*, 2013, **4**, 1125-1136.
14. A. Zaïm, S. V. Eliseeva, L. Guénée, H. Nozary, S. Petoud and C. Piguet, *Chem. Eur. J.*, 2014, **20**, 12172-12182.
15. F. Song, G. Wei, X. Jiang, F. Li, C. Zhu and Y. Cheng, *Chem. Commun.*, 2013, **49**, 5772-5774.
16. J. Yuasa, T. Ohno, H. Tsumatori, R. Shiba, H. Kamikubo, M. Kataoka, Y. Hasegawa and T. Kawai, *Chem. Commun.*, 2013, **49**, 4604-4606.
17. J. Yuasa, T. Ohno, K. Miyata, H. Tsumatori, Y. Hasegawa and T. Kawai, *J. Am. Chem. Soc.*, 2011, **133**, 9892-9902.
18. J. Yuasa, H. Ueno and T. Kawai, *Chem. Eur. J.*, 2014, **20**, 8621-8627.
19. J. L. Lunkley, D. Shirotani, K. Yamanari, S. Kaizaki and G. Muller, *Inorg. Chem.*, 2011, **50**, 12724-12732.
20. J. P. Riehl and G. Muller, in *Comprehensive Chiroptical Spectroscopy*, eds. N. Berova, P. L. Polavarapu, K. Nakanishi and R. W. Woody, Wiley, 2012, vol. 1.
21. E. Castiglioni, S. Abbate and G. Longhi, *Appl. Spectrosc.*, 2010, **64**, 1416-1419.
22. E. Castiglioni, S. Abbate, F. Lebon and G. Longhi, *Method. Appl. Fluoresc.*, 2014, **2**, 024006.
23. V. Schurig, W. Bürkle, K. Hintzer and R. Weber, *J. Chromatogr. A*, 1989, **475**, 23-44.
24. D. Shirotani, T. Suzuki and S. Kaizaki, *Inorg. Chem.*, 2006, **45**, 6111-6113.
25. J. L. Lunkley, D. Shirotani, K. Yamanari, S. Kaizaki and G. Muller, *J. Am. Chem. Soc.*, 2008, **130**, 13814-13815.
26. G. Muller, *Dalton Trans.*, 2009, 9692-9707.
27. C. Freund, W. Porzio, U. Giovanella, F. Vignali, M. Pasini, S. Destri, A. Mech, S. Di Pietro, L. Di Bari and P. Mineo, *Inorg. Chem.*, 2011, **50**, 5417-5429.
28. F. Zinna, U. Giovanella and L. Di Bari, *Adv. Mater.*, 2015, **27**, 1791-1795.
29. S. Di Pietro and L. Di Bari, *Inorg. Chem.*, 2012, **51**, 12007-12014.
30. L. Di Bari and P. Salvadori, *Coord. Chem. Rev.*, 2005, **249**, 2854-2879.
31. L. Di Bari, G. Pintacuda, S. Ripoli and P. Salvadori, *Magn. Reson. Chem.*, 2002, **40**, 396-405.
32. C.-H. Huang, *Rare earth coordination chemistry: Fundamentals and applications*, John Wiley & Sons, 2010.
33. J. I. Bruce, D. Parker, S. Lopinski and R. D. Peacock, *Chirality*, 2002, **14**, 562-567.